Quantifying Radium in Human Bone: A Novel Application of Digital Autoradiography

George Tabatadze[1], Jessica E. Linson[2], John D. Brockman[2], Sergey Y. Tolmachev[1]

[1]United States Transuranium and Uranium Registries, College of Pharmacy and Pharmaceutical Sciences, Washington State University, Richland, WA, USA

[2]Department of Chemistry, University of Missouri, Columbia, MO, USA

Introduction

An ionizing radiation quantum imaging detector (iQID) is employed at the United States Transuranium and Uranium Registries as a non-destructive technique to visualize the micro-distribution of alpha-emitting radionuclides in human tissues. This study evaluates the use of iQID not only for spatial distribution mapping but also for quantifying ^{226}Ra activity concentrations in bone samples from a historical case of a female radium dial painter.

Materials and Methods

Sample Description

Bone samples from the femur shaft and thoracic vertebra (Fig. 1) were taken from radium dial painter case 03-666, with an estimated ^{226}Ra uptake of 58.9 MBq (Rowland 1994).

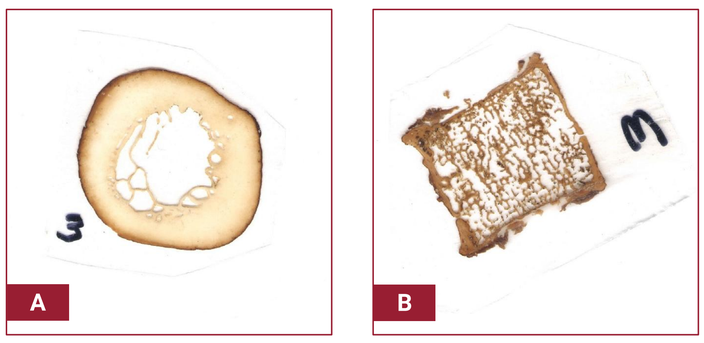

Figure 1: Plastic embedded bone sections of femur middle shaft (A) and thoracic vertebral body (B).

iQID System Setup

Samples were imaged using the iQID. A shadow image was acquired with iQID to verify source positioning and provide scale calibration. The imager's intrinsic efficiency was assessed using a NIST-traceable source containing electrodeposited ^{242}Pu, ^{239}Pu, ^{241}Am (Fig. 2). After iQID imaging, these bone sections were acid-digested and analyzed by inductively coupled plasma mass spectrometry (ICP-MS).

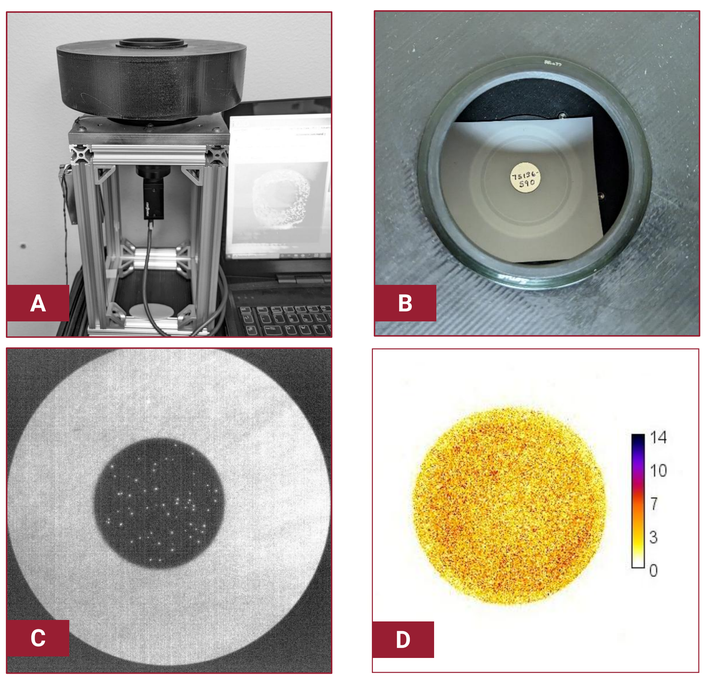

Figure 2: iQID system setup and calibration workflow: iQID assembly (A), source placement (B), shadow image acquisition (C), and iQID imaging result (D).

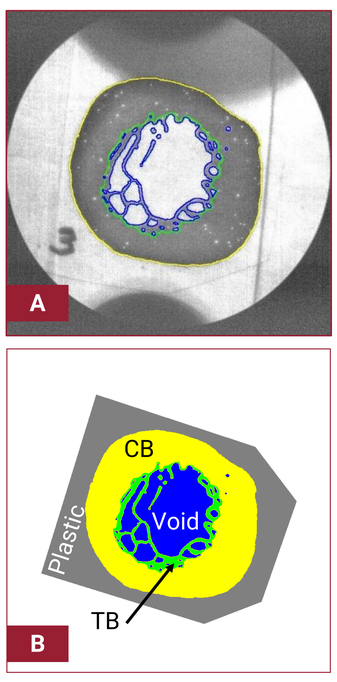

Figure 3: Shadow image acquisition (A) and ROI segmentation (B).

Image Acquisition and ROI Segmentation

iQID and shadow images of bone sections were acquired. Anatomical bone slide scans (Fig. 1) were registered with shadow images (Fig. 3) for scale and positioning, and ROIs were then segmented in ImageJ. Segmented regions included cortical bone (CB), trabecular bone (TB), plastic, and voids; CB and TB ROIs defined the ^{226}Ra source regions, while plastic and void ROIs were later applied in Monte Carlo simulations.

Geometric Efficiency Calculation

A custom Python code was developed to evaluate geometric efficiency using Monte Carlo alpha particle transport. ROI-based masks from iQID images were converted into voxelized 3D bone geometries by extending the 2D surface representation (*x*-*y*) uniformly in the *z*-direction to the slide thickness of ~150 μm (Fig. 4). A probability map of alpha emission, derived from iQID activity distributions, was applied to model non-uniform source distributions. Particles were transported through the voxelized geometry, and those reaching the detector (scintillator surface) were tallied. Geometric efficiency was calculated as the ratio of detected to emitted particles for both femur and vertebra samples. Sample masses were also estimated from the 3D geometry using the ICRP 110 bone density of 1.92 g cm^{-3} (ICRP 2009).

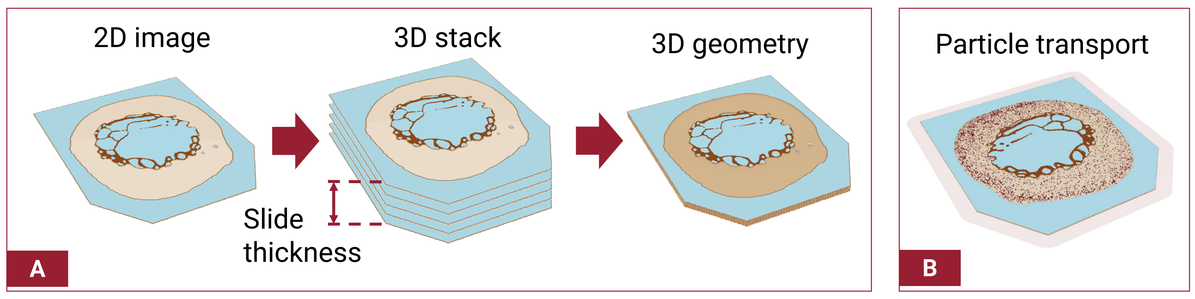

Figure 4: Construction of 3D voxelized bone geometry (A) and modeling of non-uniform activity distribution (B).

Results

iQID was calibrated and intrinsic efficiency was determined to be 92%. Alpha activity distributions were visualized (Fig. 5) and quantified using average surface activity ($\bar{A}$s) and surface activity ranges (Table 1).

Bone masses were estimated from ROI-based voxelized geometries as 0.089 g (femur shaft) and 0.057 g (vertebral body). Monte Carlo particle transport simulations yielded comparable geometric efficiencies for both samples, with ~3.4% of emitted alpha particles reaching the detector surface (Table 1).

Figure 6 shows activity concentrations of ^{226}Ra in femur and vertebra samples measured by iQID and ICP-MS in comparison with ICRP model predictions (ICRP 2017).

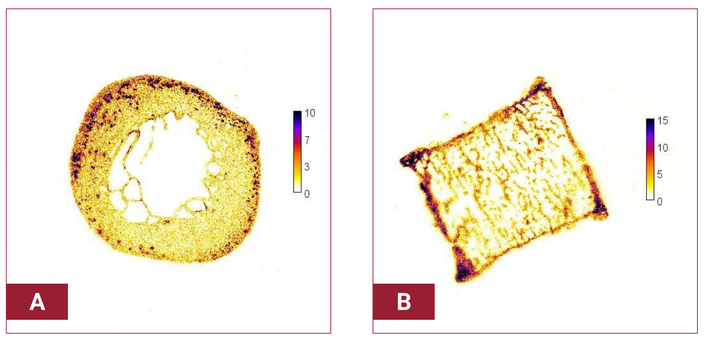

Figure 5: iQID imaging of ^{226}Ra distribution in femur shaft (A) and thoracic vertebral body (B).

Table 1: Calculated sample parameters and iQID results for ^{226}Ra in radium dial painter skeleton

Parameter	Femur shaft	Vertebral body
Bone mass (g)	0.089	0.057
Geometric efficiency (%)	3.35	3.36
Surface activity (mBq mm^{-2})		
Median (IQR)	7.0 (12)	1.5 (11)
Range (min – max)	0 – 95	0 – 52
Activity concentration (Bq g^{-1})		
*iQID**	219 ± 1	714 ± 2
ICP-MS	118 ± 14	178 ± 47
Model prediction	213	731

** Counting uncertainty*

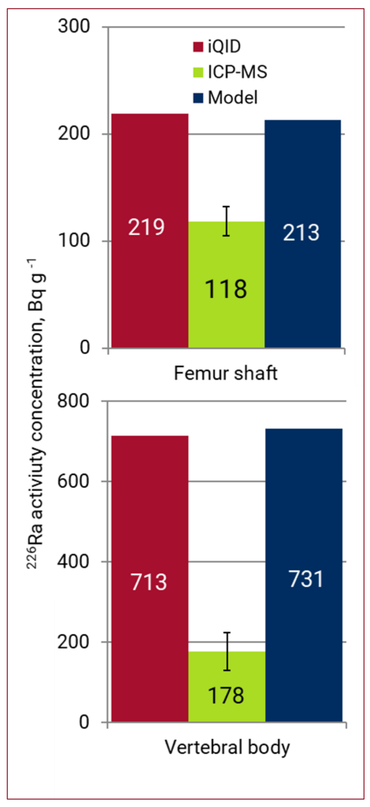

Figure 6: ^{226}Ra activity concentrations measured by iQID and ICP-MS, against ICRP model predictions.

Conclusion

- iQID-derived activity concentrations, corrected for realistic geometric efficiency, showed reasonable agreement with ICP-MS measurements and closer alignment with ICRP model predictions.
- Findings of this study highlight iQID's potential as a non-destructive tool for both spatial distribution mapping and quantification of alpha-emitting radionuclides in bone.

References

Rowland RE. Radium in humans: A review of U.S. studies; 1994

ICRP Publication 110. Annals of the ICRP 39; 2009

ICRP Publication 137. Annals of the ICRP 46; 2017

Acknowledgment

The USTUR is funded by U.S. Department of Energy, Office of Domestic and International Health Studies (EHSS-13), under grant award DE-HS0000073 to Washington State University.